Available online at www.sciencedirect.com
SCIENCE DIRECT®
Materials Research Bulletin 39 (2004) 2229–2240
Materials Research Bulletin
www.elsevier.com/locate/matresbu

Electrical properties of Mg-doped $LiTaO_3$ ceramics

A. Huanosta[a,*], E. Alvarez[b], M.E. Villafuerte-Castrejón[a], A.R. West[c]

[a]*Instituto de Investigaciones en Materiales, Universidad Nacional Autónoma de México, Apartado Postal 70-360, México D.F. 04510, México*
[b]*Universidad de Sonora, Departamento de Física, Hermosillo, Sonora, México*
[c]*Department of Engineering Materials, The University of Sheffield, Mappin Street, Sheffield S1 3JD, UK*

Received 29 April 2003; received in revised form 25 November 2003; accepted 23 August 2004

Abstract

The ac impedance of ceramic samples of Mg-doped $LiTaO_3$ has been measured over the temperature range 600–800 °C. It can be modelled by an equivalent circuit composed of a ''dielectric element'' $R_1C_1C_2$ in parallel with a ''leakage resistance'' R_2. The series component R_1C_1, represents the polarisation associated with domain reorientation: C_1 passes through a maximum at T_c at the same time as R_1 passes through an approximate minimum. C_2 represents the bulk polarisation, R_2 shows linear Arrhenius behaviour.

The solid solution were characterised by XRD and the formation mechanism was proposed. The variation of electrical properties with composition is discussed.

Keyword: A. Ceramics; A. Oxides; B. Chemical synthesis; C. X-ray diffraction; D. Crystal structure; D. Dielectric properties

1. Introduction

Lithium metatantalate, $LiTaO_3$, has various uses due to its pyroelectric, piezoelectric and electrooptic properties[1–4]. It is an apparently simple material whose crystal structure is a corundum (α-Al_2O_3) superstructure with an ordered arrangement of Li^+, Ta^{5+} cations over two-third of the octahedral sites between the hexagonal close packed layers of oxide ions. In reality, however, it is a non-stoichiometric phase, existing over the composition range ~46.0–50.4 mol% Li_2O at high temperatures and with a defect structure that is still not well understood [5–7].

* Corresponding author.

0025-5408/$ – see front matter
doi:10.1016/j.materresbull.2004.08.008

$LiTaO_3$, and the structurally-similar $LiNbO_3$, can be doped with a wide range of cations, M, that accept octahedral coordination to oxygen with M–O bond distances typically in the range 1.9–2.2 Å [8–14]. The Curie temperature of the ferroelectric–paraelectric transition is composition-dependent. Its value is ~660 °C in stoichiometric $LiTaO_3$, decreases to ~580 °C with increasing Ta content and either increases or decreases on doping with a third cation [15].

Various mechanisms for doping $LiTaO_3$ have been considered, including cation site substitutions, vacancy creation and occupation of interstitial sites. It has been proposed that, in general, the most significant doping mechanism, and the one that gives the most extensive range of solid solutions for a given dopant, is the mechanism in which the total number of cations remains constant.

In previous works [4,9,10,16,17], with different solid solutions with Ti^{4+}, Zr^{4+}, Eu^{3+}, the solid solutions were found to be the most extensive in the direction which correspond to a mechanism of constant overall cation content. Thus, for doping with, e.g. M^{2+} ions, the preferred mechanism is:

$$3Li^{+} + Nb^{5+} \leftrightarrow 4Mg^{2+} \quad (1)$$

whereas for doping with, e.g. Ti^{4+}, it is:

$$Li^{+} + 3Nb^{5+} \leftrightarrow 4Ti^{4+} \quad (2)$$

The dielectric properties of materials such as $LiTaO_3$, including the measurement of Curie temperatures, T_c, are usually investigated at a fixed frequency of 1 kHz using capacitance bridges. With such data, a permittivity maximum at a temperature corresponding to T_c is usually seen which is superposed on a curve of rapidly increasing permittivity with temperature, as shown in Fig. 1 [15].

Alternative methods for the characterisation of ferroelectric materials have been developed based on impedance spectroscopy. Instead of fixed frequency measurements, data are collected over a wide frequency range, usually covering 5–10 decades in frequency; with appropriate methods of analysis, a much more complete characterisation of the electrical properties of a ferroelectric material is possible than can be obtained from fixed frequency measurements alone.

In a previous study of a single crystal of $LiTaO_3$, the electrical properties in two crystallographic orientations were determined. Perpendicular to the polar *c*-axis, the crystal had a low, temperature-

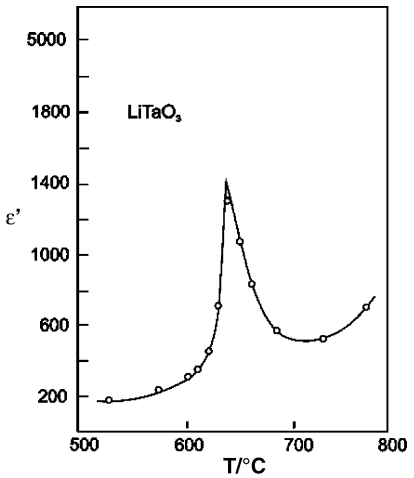

Fig. 1. Fixed frequency permittivity data for $LiTaO_3$ ceramic.

independent capacitance and a modest temperature dependent electronic conductivity. Parallel to the *c*-axis, however, the leakage conductivity appeared to be ionic—due to Li^+ ions—and the effect of this could be separated from the dielectric relaxation associated with domain reversal. Further, two capacitance parameters were determined; one, C_1, was associated with the permittivity maximum at T_c, Fig. 2; the other, C_2, corresponded to the bulk permittivity of the sample which was essentially independent of temperature. In fact C_2 exhibited slight temperature dependence just below T_c, Fig. 2. The equivalent circuit, which was found to be the most appropriate circuit to explain the experimental data, is also shown in Fig. 2 [3].

Impedance data obtained from polycrystalline materials are generally more complex than those obtained from single crystals. Thus, any effects associated with crystal anisotropy will be superposed in a given data set for a ceramic sample composed of randomly oriented grains. In addition, extra impedances associated with grain boundaries and contacts may be present. It is, nevertheless, important to investigate such situations since polycrystalline materials are often the only ones that are available. In this study, we give a preliminary report of the properties of Mg-doped $LiTaO_3$ ceramics as determined by impedance spectroscopy and compare the results with those reported in the literature.

2. Experimental

Samples of Mg-doped $LiTaO_3$ were prepared by solid state reaction. Starting materials were Li_2CO_3, MgO (both reagent grade) and Ta_2O_5 (99.99%). Reagents were weighed out to give mixtures totalling 5–10 g. These were mixed with an agate mortar and pestle for ~15 min and reacted in Pt crucibles. Initial firing was at 650 °C, to expel CO_2, followed by 1000 °C for 6 days to complete the reaction. Products were analysed by X-ray powder diffraction using a Siemens D500 diffractometer. For accurate lattice parameter determination, a slow scan speed 1/2° 2θ min^{-1} was used. For electrical property measurements, pellets of approximate dimensions 2 mm × 6 mm × 8 mm were prepared by uniaxial pressing at 5 ton cm^{-2}. These were sintered at 1000 °C, in a free atmosphere furnace. Electrodes fabricated from Au

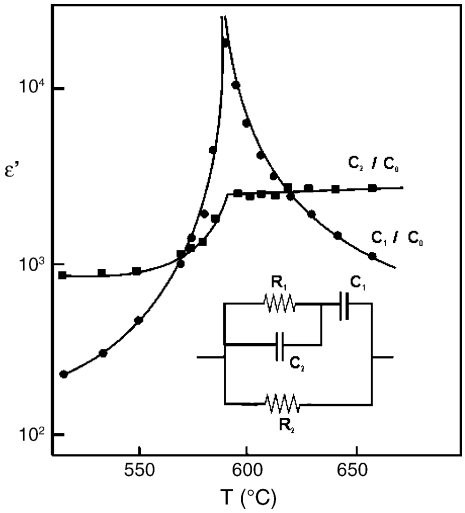

Fig. 2. Capacitance data for single crystal $LiTaO_3$ and equivalent circuit used.

paste (Johnson Matthey) were fired on at 700 °C and then attached to the leads of a conductivity jig which was placed inside a furnace whose temperature was controlled and measured to within 5 °C. For impedance measurements, a Hewlett Packard 4192 impedance analyser was used; data were collected over the frequency range 5 Hz to 13 MHz, although, in general the data above ~1 MHz were found to be unreliable. Runs were taken in 25–30 °C steps. The rms applied voltage was 1 V. Corrections for lead resistances were not necessary since these were many orders of magnitude less than those of the sample. High frequency data were corrected for the parallel "blank" capacitance of the conductivity jig which was ~10 pF.

3. Results and discussion

The area of compositions that forms $LiTaO_3$ solid solutions in the system Li_2O–MgO–Ta_2O_5 is shown in Fig. 3. The solid solutions are most extensive on the join $LiTaO_3$–$Mg_4Ta_2O_9$, corresponding to substitution mechanism (1), above. On this join (the stoichiometric join) the solid solution formula may be written: $Li_{1-3x}Mg_{4x}Ta_{1-x}O_3$: $0 < x < 0.10$. For compositions off this join, the additional mechanism, $5Li^+ \leftrightarrow Ta^{5+}$ is necessary. The solid solution area may therefore be represented by the general formula:

$$Li_{1-3x-5y}Mg_{4x}Ta_{1-x+y}O_3$$

Variation of the lattice parameters with composition on the stoichiometric join is shown in Fig. 4, *a* increases significantly with *x* and *c* shows a small increase with *x*.

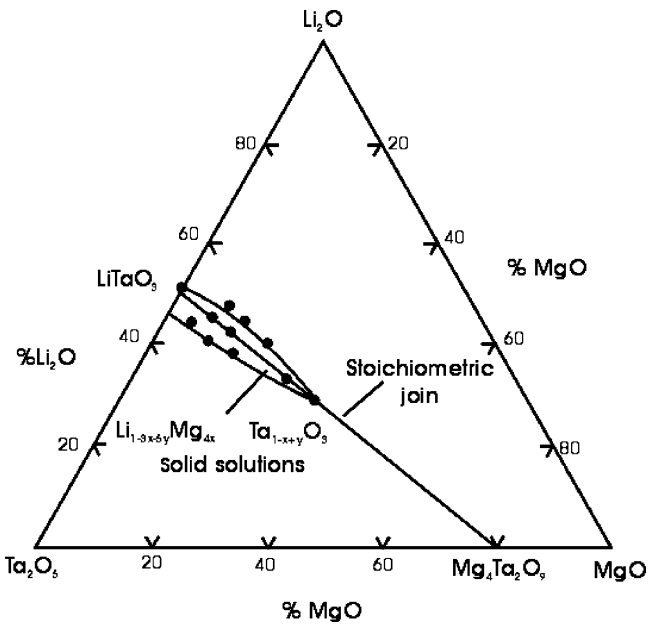

Fig. 3. Locus of Mg-doped solid solutions in the system Li_2O–MgO–Ta_2O_5.

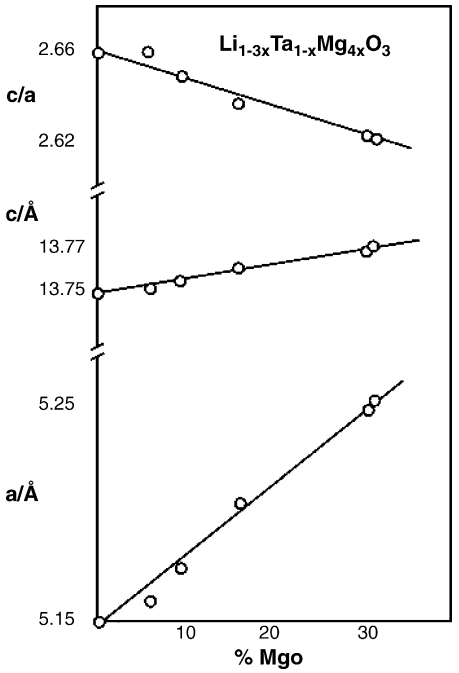

Fig. 4. Lattice parameters of $LiTaO_3$ solid solutions.

Impedance data were collected for each composition in the temperature range ~600–800 °C, with temperature steps of 25–30 °C.

Three typical data sets are shown in Fig. 5 for one composition ($x = 0.058$, $y = -0.019$) in the form of complex impedance plots Z'' versus Z'. The data generally show two poorly resolved semicircles or arcs, the resolution of which is rather temperature dependent. At low frequencies a small tail is seen. In order to analyse the impedance data we assume, for a starting model, that the equivalent circuit shown in Fig. 2 is appropriate, it should be noted that the dielectric response represented by the elements R_1, C_1 and C_2 will be dominated, in average, by those crystals oriented with the lattice parameter c in the direction of the applied ac electric field. Resistance R_2 is a leakage resistance in parallel with the dielectric response, and could correspond to conduction either $||$ to c or $\perp$ to c depending on the ceramic texture and the level of conduction anisotropy. In addition, grain boundary impedances are assumed not to be of major importance. The validity of both these assumptions is borne out by subsequent analysis.

Various approaches were tried in order to analyse the impedance data. Initially, the raw impedance data were converted to give complex admittance plane plots, Y'' versus Y'. From these, values for two of the parameters, C_2 and R_2, were readily obtained, but values for R_1 and C_1 were not easily obtained due to poor resolution in the features of the complex admittance plots.

The approach that was finally found to be successful, was to show that the circuit in Fig. 2 gave simulated impedance results that were similar to those obtained experimentally. The sequence in Fig. 5a–c, is to illustrate two extreme cases (a and c) and to show the best fit (Fig. 5b). This last is shown schematically in Fig. 6, the figure includes the relevant equations which were used for extracting values of the resistance and capacitance parameters. The general form of the experimental and calculated sets of curves is similar, especially as regards the Z' intercept values, although, the simulated data show

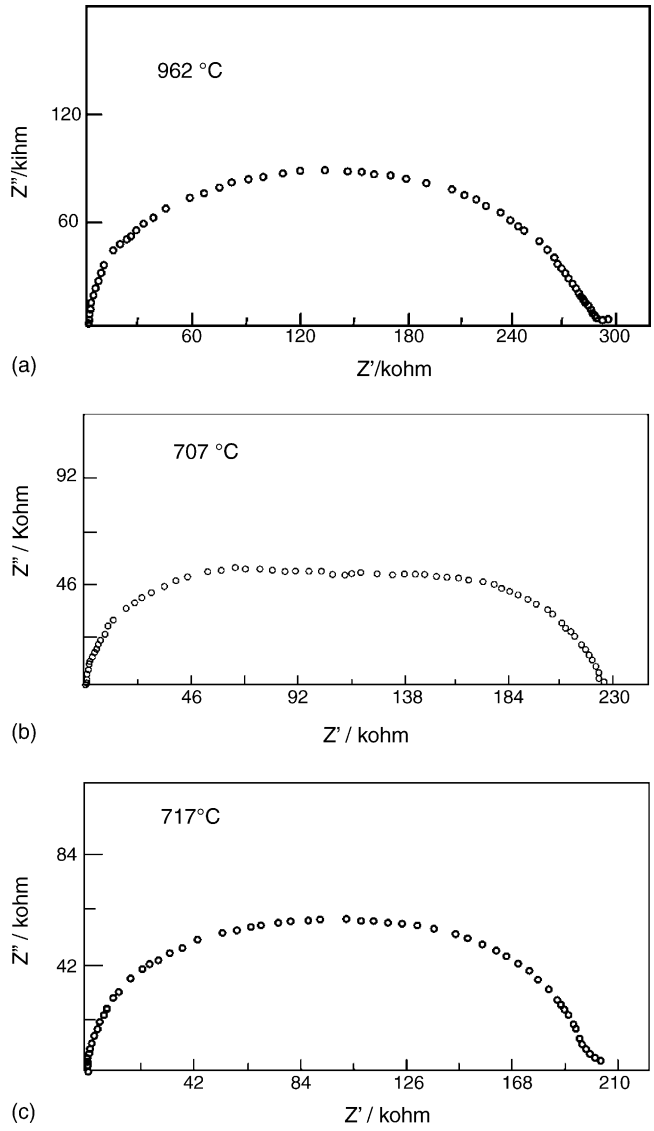

Fig. 5. Three impedance data sets for one composition: $x = 0.058$, $y = -0.019$.

semicircles that are more nearly ideal. This indicates that the true equivalent circuit may contains some non-ideal components instead of, or as well as, the frequency-independent components of Fig. 2. While the inclusion of such components is essential for a quantitative fitting to all aspects of the impedance data, their exclusion does not detract from the general validity of the resistance and capacitance values; rather, it introduces some uncertainty in the absolute values of the R and C parameters.

In the fitting shown in Figs. 5 and 6, the involved error between calculated and experimental parameters is close to 2% for R_1 and R_2, whilst it is around 3% for C_1 and C_2.

Using the methodology indicated in Fig. 6, all impedance data sets were analysed. All data sets showed a common feature in that two overlapping arcs or semicircles were present; an unusual feature is that

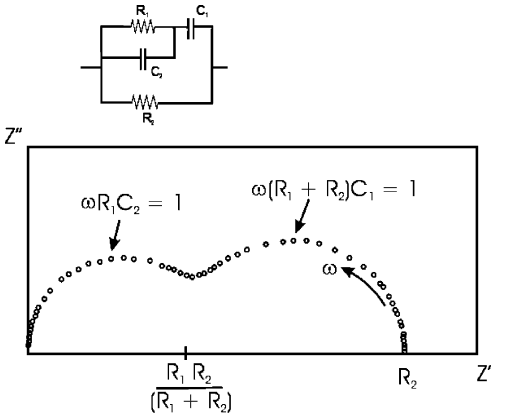

Fig. 6. Simulated impedance data for equivalent circuit shown.

these were best resolved at temperatures close to T_c, Fig. 5b. We therefore have confidence in assigning two semicircles to all data sets, even those in which the resolution is poor. From these analyses, the following conclusions were drawn: Capacitance C_1 showed a maximum in its temperature dependence, characteristic of a ferroelectric to paraelectric transition at the Curie temperature, T_c. Data for two representative compositions are shown in Fig. 7. An interesting observation is that T_c rises with increasing Mg content; this is summarised in Table 1. A plausible explanation of this correlation is that with increasing lattice parameter, the cation sites may expand. Hence, the structural distortions of the (LiO_6) and/or (TaO_6) octahedra which give rise to ferroelectricity become easier or more pronounced. Consequently, the temperature, T_c, required to eliminate the cooperative distortions of the octahedra, which give rise to the ferroelectricity in doped $LiTaO_3$, also rises.

Data for C_2 are largely temperature-independent but may show a small inflexion or increase around T_c, Fig. 8. This behaviour is rather similar to that of C_2 for single crystal $LiTaO_3$ with the ac electric field parallel to c which showed a small increase as temperature increased through T_c.

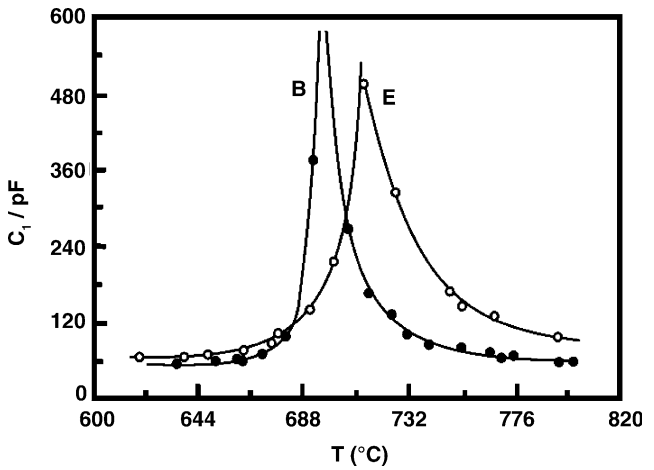

Fig. 7. Capacitance, C_1, data for two compositions.

Table 1
Compositions and some properties studied

Label	Li_2O:Ta_2O_5:MgO (mol%)	x	y	E_a (eV)	T_c (°C)
A	47:43:10	0.0275	−0.024	1.54	688
D	44:42:14	0.039	−0.0205	1.28	692
G	40:40:20	0.058	−0.019	1.60	710
C	44:51:5	0.012	0.019	1.20	688
F	40:50:10	0.025	0.025	1.27	707
H	38:47:15	0.039	0.018	1.28	695
B	45:47:8	0.021	0	1.40	696
E	42:45:13	0.035	0	1.29	718
I	33:40:27	0.078	0	1.32	733
J	29:37:34	0.103	0	1.35	765

C_2 is therefore attributed to the polarisation of the lattice, which is largely unaffected by T_c. C_1 is attributed to the polarisation of the domains (Fig. 7) and in particular, is associated with domain or domain wall reorientation.

Data for R_2, give Arrhenius plots that are generally linear, Fig. 9, with activation energies summarised in Table 1. At this stage, we do not know if the charge carriers responsible for R_2 are ionic (Li^+), electronic or a mixture. There is some evidence of a low frequency tail in the impedance data, Fig. 4, which could indicate an ionically blocking, component, but this does not develop into a proper "electrode spike" over the range of available frequencies; a definite assignment cannot be made at this stage, therefore.

Data for R_1 gave Arrhenius plots that are markedly non-linear, but pass through a resistance minimum in the region of T_c, Fig. 9b; again, there are strong similarities with the behaviour of R_1 for single crystal $LiTaO_3$—it showed an increasingly rapid decrease with increasing temperature as T_c was approached, and had a small, non-zero value at and above T_c.

R_1 is therefore attributed to the resistance associated with the same domain reorientation process that is responsible for C_1.

In Figs. 7–9, by using the deviation (%) between calculated and experimental data we estimated the associated errors, which are masked by the used symbols in the figures.

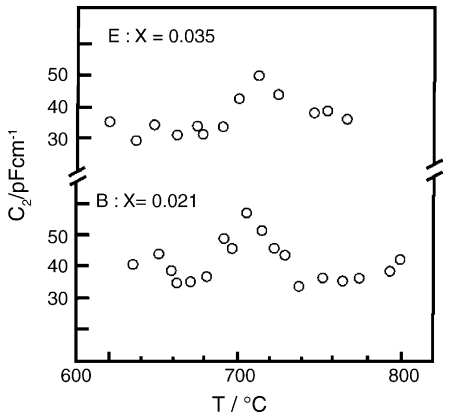

Fig. 8. Capacitance, C_2, data for two compositions.

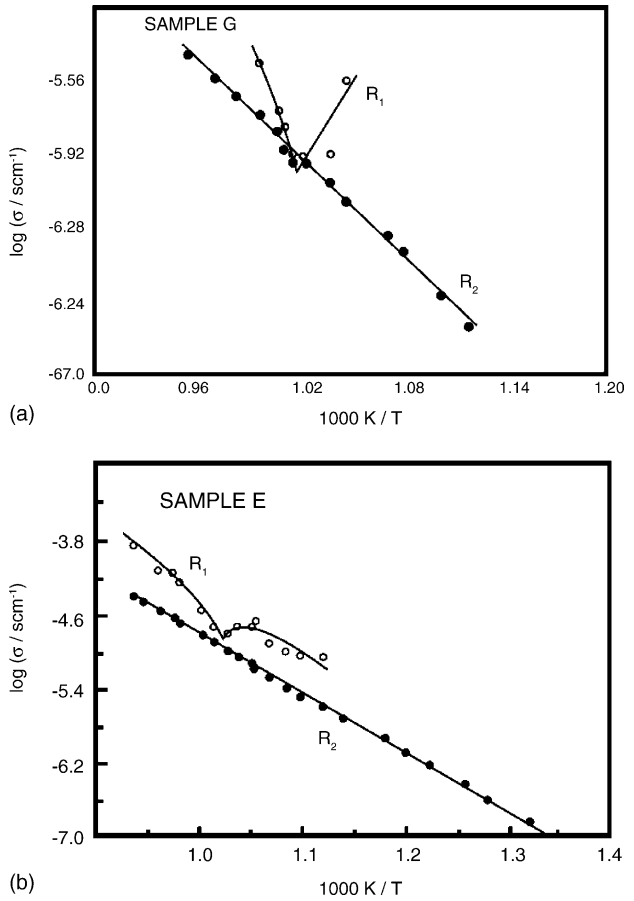

Fig. 9. Resistances, R_1 and R_2, in Arrhenius format for two compositions.

By using a scanning electron microscope (Cambridge-Leica Steroescan 440) information of the microstructure in the studied specimens was obtained. Two microphotographs, which were obtained from fractured samples, and correspond to samples B and E in Table 1 are shown in Fig. 10a and b. The shape of the grains tends to be spherical in both cases. The microstructure of these samples is quite similar for all studied compounds. The grain size distribution, which was observed in the back-scattering image of B is approximately in the range 1–5 μm. Fig. 10b shows a microphotograph of sample E at equal magnification than the former ones. There is a small tendency to increase the grain size for large Mg contents, however we point that much more homogeneous grain size is obtained at increasing Mg concentrations. In the case of 27% Mg (sample I) for example, the average grain size was found to be 2.1 μm.

4. Conclusions

Impedance spectroscopy provides a powerful technique for the characterisation of doped $LiTaO_3$ ceramics over a range of temperatures spanning the ferroelectric to paraelectric transition. The

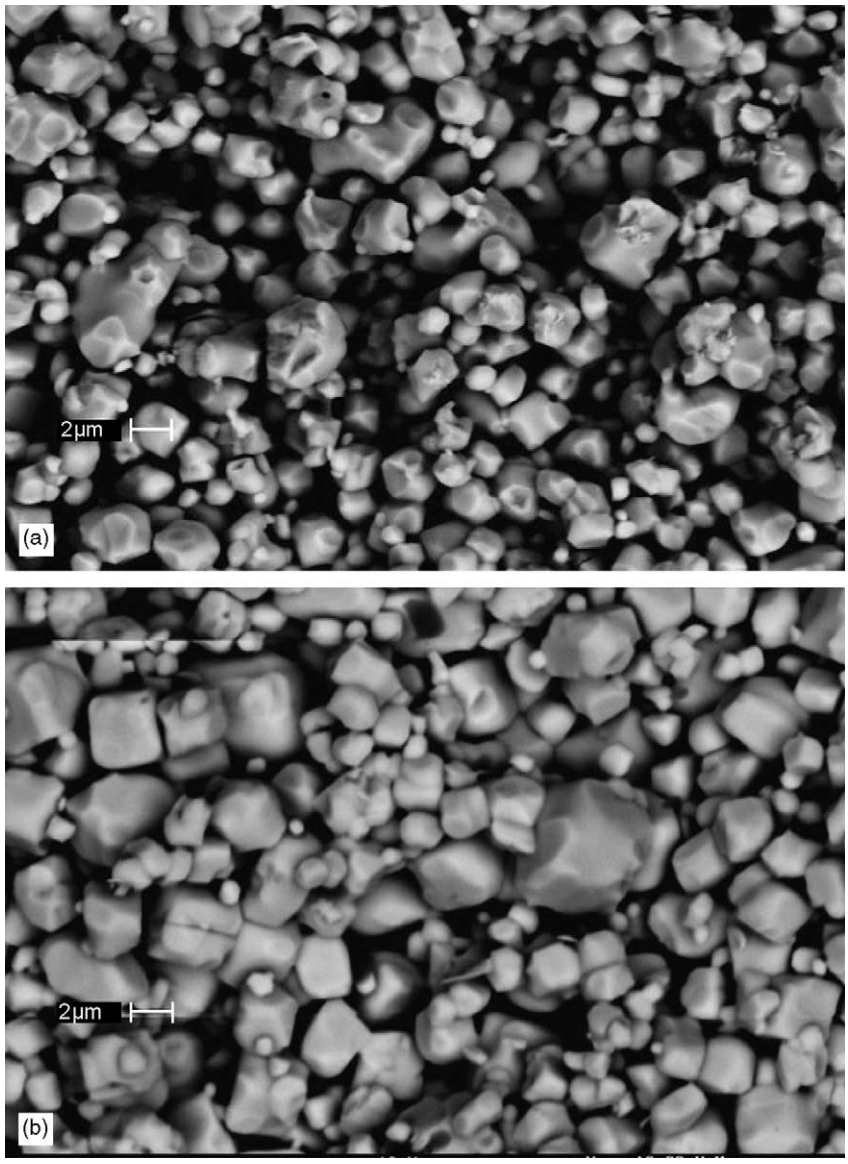

Fig. 10. (a) SEM image of the B sample taken from a fractured specimen. (b) Backscattering image of the E sample containing 13% Mg.

impedance data are broadly similar to those obtained for single crystal $LiTaO_3$ with the ac electric field applied parallel to the *c* axis and can be analysed using the same equivalent circuit, composed of a dielectric relaxation component in parallel with a leakage resistance. A simplified method of analysis is developed which gives values for the component *R* and *C* parameters directly from the impedance data.

The Mg-doped $LiTaO_3$ ceramics show a modest level of leakage conductivity which may be either ionic or electronic, with a linear Arrhenius temperature dependence and no evidence of deviation or

discontinuity at T_c. There is no evidence for significant grain boundary impedances: the entire response is attributed to the ceramic bulk.

The impedance data of the doped $LiTaO_3$ ceramics show a consistent and unusual feature that, to our knowledge, has not been observed in the ac response of any other electrical material. In this, the impedance data at all temperatures correspond to two poorly-resolved and overlapping semicircles, but the degree of resolution does improve significantly for a small range of temperatures around T_c. We attribute this to the fact that capacitance C_1 shows a large variation in the region of T_c. In particular, $C_1 \gg C_2$ close to T_c. Consequently the relaxation times of the two impedance semicircles, given by R_1C_2 and $(R_1 + R_2)C_1$, diverge in the region of T_c. Since the semicircle maxima occur at frequencies given by the general relation: $\omega_{max} RC = 1$, the resolution of the two semicircles depends on their having significantly different ω-values; hence, because of the nature of the dramatic variations in C_1 with temperature, the resolution of the two impedance semicircles is greatest at T_c.

The dielectric properties of doped $LiTaO_3$ ceramics can be represented by the same R_1, C_1, C_2 circuit components that were used to represent single crystal $LiTaO_3$. The capacitance, C_1, with its characteristic temperature dependence, provides the usual means for describing permittivity data. In addition, the parameter R_1 provides complementary information on the resistance associated with the domain reorientation.

Thus, R_1 tends to pass through a minimum at the same time as C, passes through a maximum.

The transition temperature, T_c, of the Mg-doped $LiTaO_3$ solid solutions shows a significant increase with increasing Mg content. At the same time, the lattice parameters and unit cell volume also increase significantly with Mg content. A ready explanation of this correlation is that with increasing lattice parameter, the cation sites also expand. Hence, the structural distortions of the (LiO_6) and/or (TaO_6) octahedra which give rise to ferroelectricity become easier or more pronounced. Consequently, the temperature, T_c, required to eliminate the cooperative distortions of the octahedra, which give rise to the ferroelectricity in doped $LiTaO_3$, also rises.

Acknowledgements

We would like to thank R. Reyes and L. Baños for their technical assistance. We also thank DGAPA (UNAM) for support through the PAPIIT program No. IN103603 and IN-113814/15.

References

[1] Rauber, Chemistry and Physics of Lithium Niobate, Current Topics in Materials Science, vol. I, North Holland Publication Co., 1978.
[2] J. Ravez, G.T. Joo, J.P. Bonnet, Ferroelectrics 81 (1988) 305.
[3] D.C. Sinclair, A.R. West, Phys. Rev. B 39 (18) (1989) 13486.
[4] M.E. Villafuerte-Castrejón, A.R. West, J. Rubio O., Radiat. Eff. Defects Solids 114 (1990) 175.
[5] L.O. Svaasand, M.E. Riksrud, G. Nakken, A.P. Grande, F. MO, J. Cryst. Growth 18 (1973) 179.
[6] R.S. Roth, H.S. Parker, W.S. Brower, J.L. Waring, in: W. Van Gool (Ed.), Phase Equilibria, Crystal Chemistry and Crystal Growth of Alkali Oxide–Metal Oxide Systems, North Holland, 1973, p. 217.
[7] P. Lerner, C. Legras, P. Dumas, J. Cryst. Growth 34 (1968) 23l.
[8] B. Elouadi, M. Zrioull, J. Ravez, P. Hagenmuller, Ferroelectrics 38 (1981) 793.

[9] M.E. Villafuerte-Castrejón, A. Aragon-Piña, R. Valenzuela, A.R. West, J. Solid State Chem. 71 (1987) 103.
[10] M.E. Villafuerte-Castrejón, C. Kuhliger, R. Ovando, R.I. Smith, A.R. West, J. Mater. Chem. 1 (1991) 747.
[11] S. Kawakami, A.T. Suzuki, T. Sekiya, T. Ishikuro, M. Masuda, Y. Torii, Mater. Res. Bull. 20 (1985) 1435.
[12] B. Elouadi, E. Lotfi, J. Solid State Chem. 67 (1987) 308.
[13] Y. Torii, I.T. Sekiya, T. Yamamoto, K. Kayabashi, Y. Abe, Mater. Res. Bull. 18 (1983) 1569.
[14] G.T. Joo, J. Senegas, J. Ravez, P. Hagenmuller, J. Solid State Chem. 68 (1987) 247.
[15] A. Huanosta, A.R. West, J. Appl. Phys. 61 (1987) 5386.
[16] M.E. Villafuerte-Castrejón, R. Valenzuela, A.R. West, in: P. Vicenzini (Ed.), High Tech Ceramics, Elsevier, 1987, p. 1611.
[17] M.E. Villafuerte-Castrejón, A.R. West, A. Muñoz, O. J. Rubio, Radiat. Eff. Defects Solids 124 (1992) 341.